Supplementary Material:

Crystal Chemistry and Thermodynamic Properties of Zircon Structure-Type Materials

Andrew C. Strzelecki[1,2,3,4], Xiaodong Zhao[1,2], Paul Estevenon[5], Hongwu Xu[4,6], Nicolas Dacheux[7], Rodney C. Ewing[8], Xiaofeng Guo[1,2,3,9,*]

[1] *Department of Chemistry, Washington State University, Pullman, Washington 99164, United States*

[2] *Alexandra Navrotsky Institute for Experimental Thermodynamics, Washington State University, Pullman, Washington 99164, United States*

[3] *Materials Science and Engineering, Washington State University, Pullman, Washington 99164, United States*

[4] *Earth and Environmental Sciences Division, Los Alamos National Laboratory, Los Alamos, New Mexico 87545, United States*

[5] *CEA, DES, ISEC, DMRC, Univ Montpellier, Marcoule, 30207, France*

[6] *School of Molecular Sciences, Center for Materials of the Universe, Arizona State University, Tempe, Arizona 85287, United States*

[7] *ICSM, Univ Montpellier, CNRS, CEA, ENSCM, Site de Marcoule, Bagnols sur Ceze, 30207, France*

[8] *Department of Geological Sciences, Stanford University, Stanford, California 94305, United States*

[9] *School of the Environment, Washington State University, Pullman, Washington 99164, United States*

[*] e-mail: x.guo@wsu.edu

Methods of investigation into zircon-type compounds

Powder X-ray diffraction Studying the crystallographic structure with the help of powder X-ray diffraction, will lead to a pattern where the strongest diffraction peaks correspond, in descending order, to the following crystallographic planes: (200), (112), (312), and (101). The precise position of these XRD peaks will change as a result of the exact crystal chemistry of the zircon structure owing to changes in the size of the unit-cell (Figure S1). These shifts tend to be systematic across an entire series of compounds, such as with xenotimes (Ni et al. 1995; Ushakov et al. 2001a), resulting in a linear shift in unit cell parameters. This can be used further in both single substituted solid solutions, where only the lanthanide element is replaced (*i.e.,* $Er_xYb_{1-x}PO_4$) (Strzelecki et al. 2022) and in coupled substitution of solid solutions in which cations and anions are replaced, such as in phospho-silicates solid solutions ($Th_xEr_{1-x}(SiO_4)_x(PO_4)_{1-x}$) (Mesbah et al. 2016; Shelyug et al. 2021), as a means of determining the chemical composition. The reason for this is that zircon-type solid solutions follow Vegard's law. However, according to the work of Marcial et al. (2021) there are unique circumstance for which Vegard's law is not applicable, *e.g.,* for the uranothorite solid solution that exhibits a negative deviation from Vegard's law.

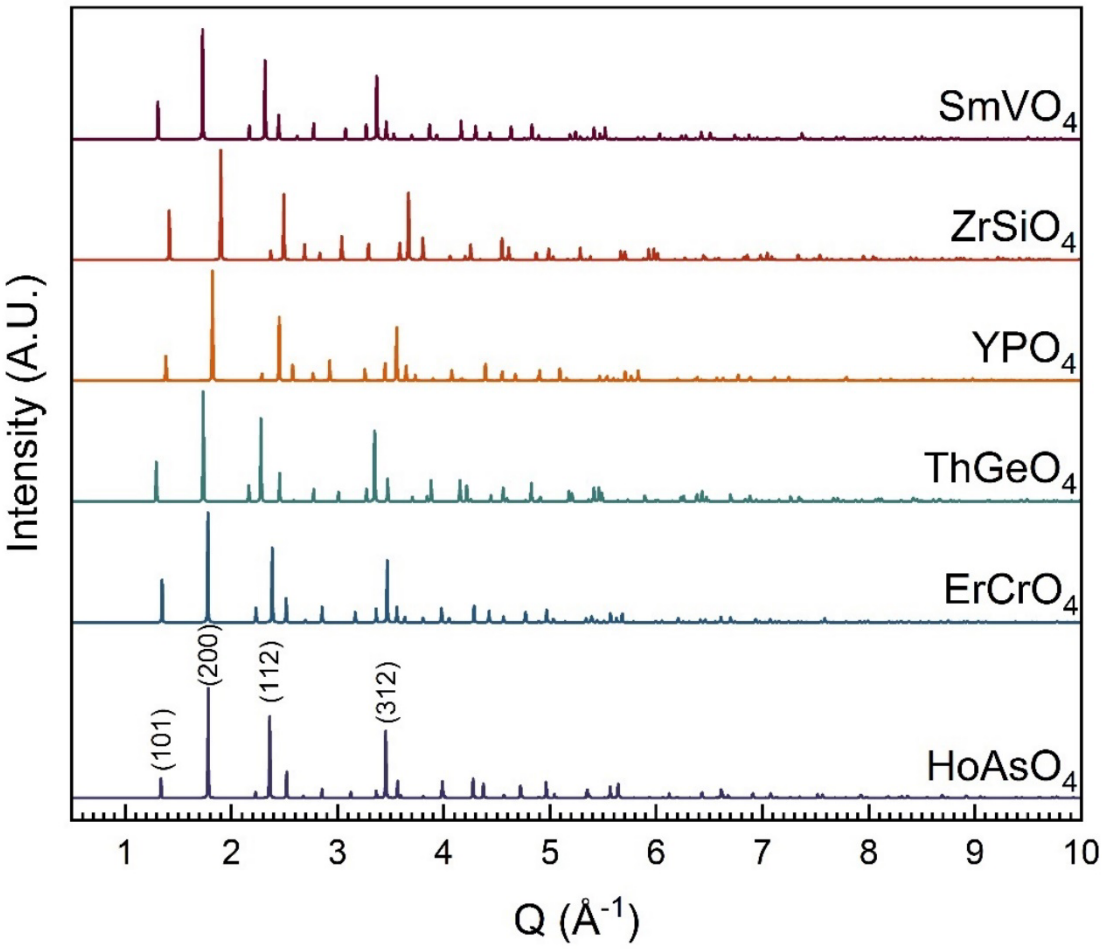

Figure S1. Calculated powder X-ray diffraction patterns for a variety of zircon structure materials, with the four strongest reflections labeled. Plots were calculated using the VESTA 3 software package (Momma and Izumi 2011) and crystallographic information files (CIFs) reported in the literature for each compound (Robinson et al. 1971; Ni et al. 1995; Mullica et al. 1996; Jiménez et al. 2002b; Schmidt et al. 2005; Achary et al. 2007).

Raman. As zircon structure-type phases belong to the D_{4h} point group, they have twelve active Raman vibrational modes, which can be determined by factor-group analysis (Dawson et al. 1971; Kolesov et al. 2001; Clavier et al. 2014). For Raman spectroscopy, seven ($\Gamma_{int} = 2A_{1g} +$

$2B_{1g} + B_{2g} + 2E_g$) (Dawson et al. 1971; Kolesov et al. 2001) can be assigned to the internal vibrations of the TO_4 tetrahedron, while the remaining five ($\Gamma_{int} = 2B_{1g} + 3E_g$) (Dawson et al. 1971; Kolesov et al. 2001) can be assigned to the external vibrations of the TO_4 tetrahedron (Dawson et al. 1971; Hoskin and Rodgers 1996; Kolesov et al. 2001). Due to the interaction of the TO_4 tetrahedra with the MO_8 dodecahedra, the tetrahedra cannot be considered as strictly independent units (Syme et al. 1977), and so there are no reported spectra with all twelve active Raman modes for zircon-type phases (Clavier et al. 2014). Instead, the visible Raman modes can be divided into three zones of interest: zone one, 900 – 1200 cm^{-1}; zone two, 350 – 900 cm^{-1}; and zone three, 100-500 cm^{-1} (Figure S2a). In the first zone, the T-O stretching motions are observed and assigned as the symmetric stretching (ν_1 - A_{1g}) and the anti-symmetric stretching (ν_3 – B_{1g}) modes. In the second zone, the T-O bending motions are observed and assigned as the symmetric bending mode (ν_2 - A_{1g}) and antisymmetric bending mode (ν_4). The third zone corresponds to the lattice vibrational modes. There is still controversy over the assignment of some of the lattice motions as well as the antisymmetric bending modes (ν_4). For a more in-depth discussion, the reader may refer to the work of Nasdala et al. (2003). A number of the zircon structure materials containing f-elements, which have been studied by Raman, can either exhibit fluorescence (i.e., U^{4+}) or display photoluminescence (i.e., REE^{3+}) (Bauer et al. 2014; Clavier et al. 2014; Lenz et al. 2015, 2019; Strzelecki et al. 2021). There are a number of advantages of using these "artifacts" (Lenz et al. 2015, 2019, 2020).

Fourier transform infrared spectroscopy (FITR). For FTIR, the $I4_1/amd$ space group induces seven active FTIR vibrational modes, which was determined again through a factor-group analysis (Dawson et al. 1971; Clavier et al. 2014). Similar to Raman spectroscopy, these

vibrational modes can be assigned to the internal and external vibrations of the SiO_4 tetrahedron. Of the seven vibrational modes, several of them ($\Gamma_{int} = 2A_{2u} + 2_{Eu}$) can be assigned to internal vibrational modes and the others ($\Gamma_{ext} = A_{2u} + 2_{Eu}$) can be assigned to external vibrational modes. Again, like with Raman, the active modes in FTIR spectra can be grouped into three zones of interest: zone one, 800 – 1200 cm^{-1}; zone two, 400 – 800 cm^{-1}, and zone three,100-400 cm^{-1} (Figure S2b). As only the antisymmetric internal modes of the TO_4 tetrahedron are visible by IR, this means that the doubly degenerated antisymmetric stretching mode (ν_3 – E_u) and the antisymmetric stretching mode (ν_3 – A_{2u}) would appear in the first zone. In the second zone, the antisymmetric deformation mode (ν_4 - A_{2u}) and the doubly degenerated antisymmetric deformation mode (ν_4 - E_u) are visible. In the third zone, the three external vibrational modes ($\Gamma_{ext} = A_{2u} + 2_{Eu}$) can be observed. However, unlike with Raman many of these vibrational modes are quite broad. The recent work reported by Clavier *et al.* (2014, 2018), on uranothorite and gadolinium orthophosphate demonstrate how to differentiate the components assigned to symmetric and antisymmetric stretching vibration modesClick or tap here to enter text.. One advantage of utilizing FTIR over Raman is when studying the simultaneous cationic and anionic solid solutions, such as with phosphor-silicate solid solutions ($Th_xEr_{1-x}(SiO_4)_x(PO_4)_{1-x}$) (Mesbah et al. 2016), one can see the effects of stretching of both TO_4 sites. For more in-depth discussion we invite the reader to the works of Nasdala et al. (2003).

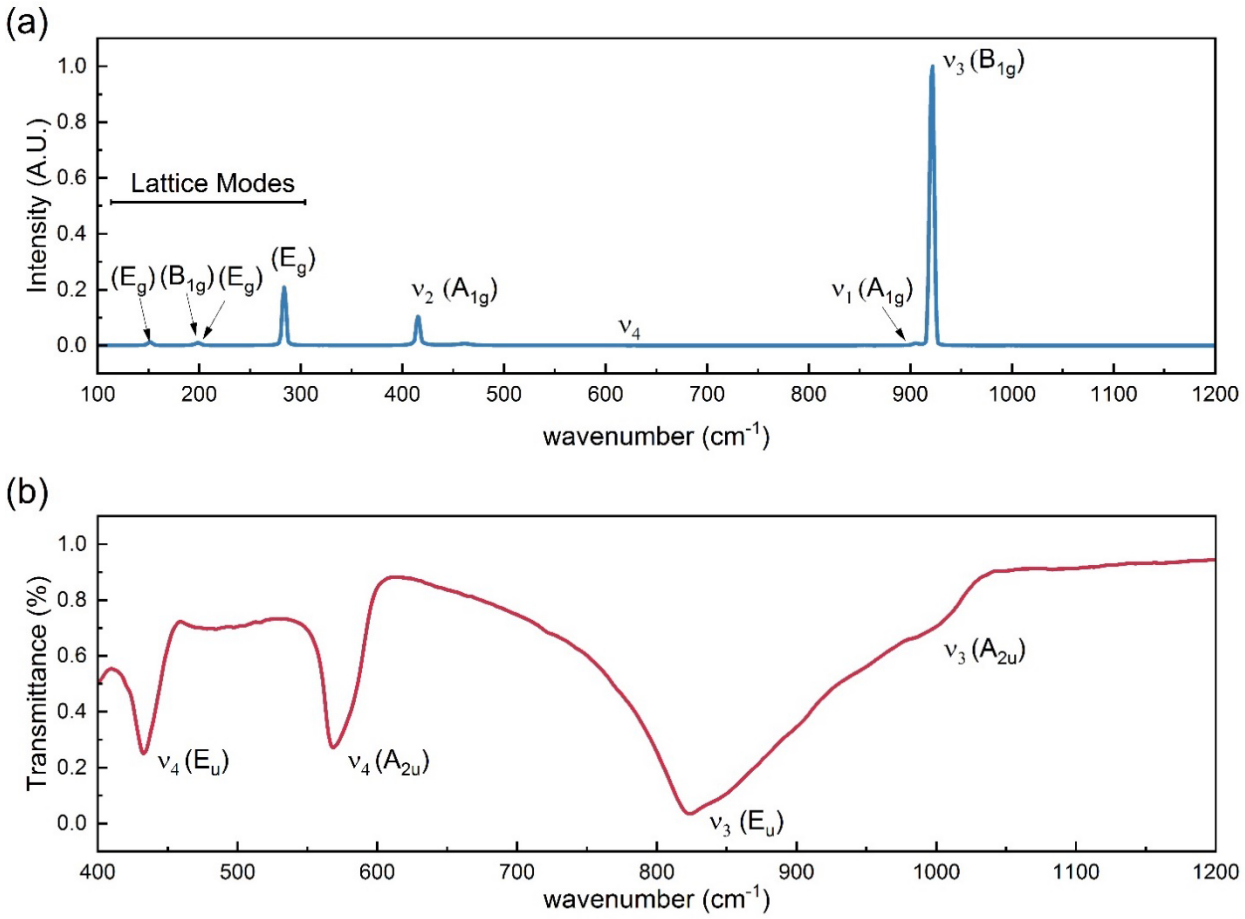

Figure S2. Representative vibrational spectra, **(a)** Raman and **(b)** FTIR, for a zircon structure material ($CeSiO_4$) (Strzelecki et al. 2021). The Raman was collected with a 532 nm laser and the FTIR was collected by Attenuated Total Reflectance.

Enthalpy (Δ*H*). There are direct and indirect experimental methods for determining the ΔH_f value of a condensed phase material, such as calorimetric techniques (*i.e.,* acid, bomb, and oxide melt), and solubility measurements. In a direct calorimetric method, heat required for forming a material is measured. For indirect calorimetric methods, heat of a given reaction (*i.e.,* dissolution or leaching, including or not oxidative processes) of the interested material is measured and used

in thermochemical cycles based on Hess's law for deriving ΔH_f. As previously stated in the introduction, zircon-type materials are highly refractory and resistant to alteration in many conditions, making the techniques based on acid or bomb calorimetry extremely difficult to implement. On the other hand, high temperature oxide melt drop solution calorimetry (Holm and Kleppa 1967; Navrotsky and Kleppa 1967), benefiting from the readily dissolution of refractory materials in high temperature oxide melts (lead borate, $PbO{\cdot}B_2O_3$ and sodium molybdate, $3Na_2O{\cdot}4MoO_3$), is one principal method to determine ΔH_f of zircon-type materials. In this technique, a small sample (~5 mg) is dropped into oxide melt of either $PbO{\cdot}B_2O_3$ or $3Na_2O{\cdot}4MoO_3$ as hot solvent maintaining at 973 K or 1073 K (Navrotsky 1977a, 1977b, 1997, 2014). Another technique used to derive ΔH_f is based on the vaporization using the mass spectrometric method in combination with Knudsen effusion (Costa et al. 2017; Kowalski et al. 2021). When studying xenotime and monazite based samples, cautious validation, however, may be needed for such refractory type materials, due to the possible formation of gaseous products during vaporization and the formation of oxyphosphates during the decomposition of the rare earth orthophosphates (Ushakov et al. 2001b).

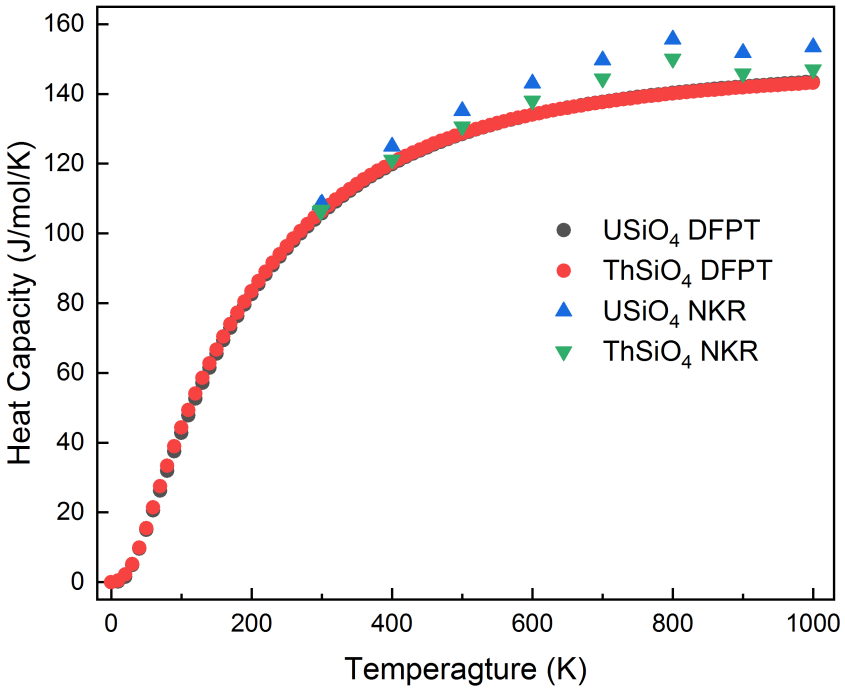

Figure S3. Constant volume heat capacity evaluated by Neumann Kopp's rule and DFT calculations.

References:

Achary, S.N., Patwe, S.J., Krishna, P.S.R., Sindhe, A.B., and Tyagi, A.K. (2007) Crystal structure analysis of Scheelite and Zircon type thorium germanates: A neutron diffraction study. Journal of Alloys and Compounds, 438, 274–278.

Armbruster, A. (1976) Infrared reflection studies on the phosphates, arsenates and vanadates of lutetium and yttrium. Journal of Physics and Chemistry of Solids, 37, 321–327.

Bandiello, E., Errandonea, D., González-Platas, J., Rodríguez-Hernández, P., Muñoz, A., Bettinelli, M., and Popescu, C. (2020) Phase behavior of $TmVO_4$ under hydrostatic compression: an experimental and theoretical study. Inorganic Chemistry, 59, 4882–4894.

Bauer, J.D., Labs, S., Weiss, S., Bayarjargal, L., Morgenroth, W., Milman, V., Perlov, A., Curtius, H., Bosbach, D., Zänker, H., and others (2014) High-pressure phase transition of coffinite, $USiO_4$. Journal of Physical Chemistry C, 118, 25141–25149.

Bayer, G. (1972) Thermal expansion of ABO_4-compounds with zircon- and scheelite structures. Journal of The Less-Common Metals, 26, 255–262.

Bose, P.P., Mittal, R., and Chaplot, S.L. (2009) Lattice dynamics and high pressure phase stability of zircon structured natural silicates. Physical Review B - Condensed Matter and Materials Physics, 79, 1–8.

Chakoumakos, B.C., Abraham, M.M., and Boatner, L.A. (1994) Crystal structure refinements of zircon-type MVO_4 (M = Sc, Y, Ce, Pr, Nd, Tb, Ho, Er, Tm, Yb, Lu). Journal of Solid State Chemistry.

Climent, E., Gallardo, J.M., de Paz, J.R., Taira, N., and Puche, R.S. (2009) Phase transition induced by pressure in $TbCrO_4$ oxide: Relationship structure-properties. Journal of Alloys and Compounds, 488, 524–527.

Climent-Pascual, E., Romero de Paz, J., Gallardo-Amores, J.M., and Sáez-Puche, R. (2007) Ferromagnetism vs. antiferromagnetism of the dimorphic $HoCrO_4$ oxide. Solid State Sciences, 9, 574–579.

Crocombette, J.P., and Ghaleb, D. (1998) Modeling the structure of zircon ($ZrSiO_4$): empirical potentials, ab initio electronic structure. Journal of Nuclear Materials, 257, 282–286.

Darnley, A.G., English, T.H., Sprake, O., Preece, E.R., and Avery, D. (1965) Ages of uraninite and Coffinite from south-west England. Mineralogical Magazine and Journal of the Mineralogical Society, 34, 159–176.

Demartin, F., Diella, V., Gramaccioli, C.M., and Pezzotta, F. (2001) Schiavinatoite, $(Nb,Ta)BO_4$, the Nb analogue of behierite. European Journal of Mineralogy, 13, 159–165.

Ding, Z., Ridley, M., Deijkers, J., Liu, N., Hoque, M.S. Bin, Gaskins, J., Zebarjadi, M., Hopkins, P., Wadley, H., Opila, E., and others (2020) The thermal and mechanical properties of hafnium orthosilicate: Experiments and first-principles calculations. Materialia, 12, 100793.

Dorogova, M., Navrotsky, A., and Boatner, L.A. (2007) Enthalpies of formation of rare earth orthovanadates, $REVO_4$. Journal of Solid State Chemistry, 180, 847–851.

Ehlers, A.M., Zaffiro, G., Angel, R.J., Boffa-Ballaran, T., Carpenter, M.A., Alvaro, M., and Ross, N.L. (2022) Thermoelastic properties of zircon: Implications for geothermobarometry. American Mineralogist, 107, 74–81.

Ellison, A.J.G., and Navrotsky, A. (1992) Enthalpy of formation of zircon. Journal of the American Ceramic Society, 75, 1430–1433.

Ennaciri, A., Kahn, A., and Michel, D. (1986) Crystal structures of $HfGeO_4$ and $ThGeO_4$ germanates. Journal of The Less-Common Metals, 124, 105–109.

Errandonea, D., and Garg, A.B. (2018) Recent progress on the characterization of the high-pressure behaviour of AVO_4 orthovanadates. Progress in Materials Science, 97, 123–169.

Errandonea, D., and Manjón, F.J. (2008) Pressure effects on the structural and electronic properties of ABX_4 scintillating crystals. Progress in Materials Science, 53, 711–773.

Errandonea, D., Lacomba-Perales, R., Ruiz-Fuertes, J., Segura, A., Achary, S.N., and Tyagi, A.K. (2009) High-pressure structural investigation of several zircon-type orthovanadates. Physical Review B - Condensed Matter and Materials Physics, 79, 1–9.

Errandonea, D., Kumar, R.S., Achary, S.N., and Tyagi, A.K. (2011) In situ high-pressure synchrotron x-ray diffraction study of $CeVO_4$ and $TbVO_4$ up to 50GPa. Physical Review B - Condensed Matter and Materials Physics, 84, 1–8.

Errandonea, D., Popescu, C., Achary, S.N., Tyagi, A.K., and Bettinelli, M. (2014) In situ high-pressure synchrotron X-ray diffraction study of the structural stability in $NdVO_4$ and $LaVO_4$. Materials Research Bulletin, 50, 279–284.

Estevenon, P., Welcomme, E., Szenknect, S., Mesbah, A., Moisy, P., Poinssot, C., and Dacheux, N. (2019a) Preparation of $CeSiO_4$ from aqueous precursors under soft hydrothermal conditions. Dalton Transactions, 48, 7551–7559.

Estevenon, P., Kaczmarek, T., Vadot, F., Dumas, T., Solari, P.L., Welcomme, E., Szenknect, S., Mesbah, A., Moisy, P., Poinssot, C., and others (2019b) Formation of $CeSiO_4$ from cerium (III) silicate precursors. Dalton Transactions, 48, 10455–10463.

Fuchs, L.H., and Gebert, E. (1958) X-ray studies of synthetic coffinite, thorite, and uranothorites. American Mineralogist, 43, 243–248.

Fuhrmann, J., and Pickardt, J. (1986) Bildung von $HfSiO_4$-Einkristallen durch chemische Transportreaktion. ZAAC - Journal of Inorganic and General Chemistry, 532, 171–174.

Garg, A.B., and Errandonea, D. (2015) High-pressure powder x-ray diffraction study of $EuVO_4$. Journal of Solid State Chemistry, 226, 147–153.

Garg, A.B., Rao, R., Sakuntala, T., Wani, B.N., and Vijayakumar, V. (2009) Phase stability of $YbVO_4$ under pressure: In situ x-ray and Raman spectroscopic investigations. Journal of Applied Physics, 106.

Garg, A.B., Shanavas, K. V., Wani, B.N., and Sharma, S.M. (2013) Phase transition and possible metallization in $CeVO_4$ under pressure. Journal of Solid State Chemistry, 203, 273–280.

Garg, A.B., Errandonea, D., Rodríguez-Hernández, P., López-Moreno, S., Muñoz, A., and Popescu, C. (2014) High-pressure structural behaviour of $HoVO_4$: Combined XRD experiments and ab initio calculations. Journal of Physics Condensed Matter, 26.

Gavrichev, K.S., Smirnova, N.N., Gurevich, V.M., Danilov, V.P., Tyurin, A. V., Ryumin, M.A., and Komissarova, L.N. (2006) Heat capacity and thermodynamic functions of $LuPO_4$ in the range 0-320 K. Thermochimica Acta, 448, 63–65.

Gavrichev, K.S., Ryumin, M.A., Tyurin, A. V., Gurevich, V.M., and Komissarova, L.N. (2010a) Heat capacity and thermodynamic functions of pretulite $ScPO_4$(c) at 0-1600 K. Geochemistry International, 48, 390–397.

——— (2010b) Heat capacity and thermodynamic functions of xenotime YPO_4(c) at 0-1600 K. Geochemistry International, 48, 932–939.

——— (2010c) Heat capacity and thermodynamic functions of YVO_4 in the 13-347 K region. Russian Journal of Inorganic Chemistry, 55, 1935–1939.

——— (2011) Revised heat capacity and thermodynamic functions of $GdVO_4$. Inorganic Materials, 47, 1120–1125.

Gavrichev, K.S., Ryumin, M.A., Tyurin, A. V., Gurevich, V.M., Khoroshilov, A. V., and Komissarova, L.N. (2012a) Thermodynamic functions of erbium orthophosphate $ErPO_4$ in the temperature range of 0-1600 K. Thermochimica Acta, 535, 1–7.

Gavrichev, K.S., Ryumin, M.A., Tyurin, A. V., Gurevich, V.M., Solov'ev, O.I., and Komissarova, L.N. (2012b) Thermodynamic functions of $ScVO_4$ at temperatures from 0 to 350 K. Inorganic Materials, 48, 845–850.

Gavrichev, K.S., Ryumin, M.A., Tyurin, A. V., Gurevich, V.M., Nikiforova, G.E., and Komissarova, L.N. (2013) Heat capacity and thermodynamic functions of $YbPO_4$ from 0 to 1800 K. Inorganic Materials, 49, 701–708.

Gavrichev, K.S., Ryumin, M.A., Gurevich, V.M., and Tyurin, A. V. (2014) Low-temperature heat capacity and thermodynamic functions of $DyVO_4$. Inorganic Materials, 50, 917–923.

Golbs, S., Cardoso-Gil, R., and Schmidt, M. (2009) Crystal structure of europium arsenate, $EuAsO_4$. Zeitschrift fur Kristallographie - New Crystal Structures, 224, 169–170.

Gomis, O., Lavina, B., Rodríguez-Hernández, P., Muṅoz, A., Errandonea, R., Errandonea, D., and Bettinelli, M. (2017) High-pressure structural, elastic, and thermodynamic properties of zircon-type $HoPO_4$ and $TmPO_4$. Journal of Physics Condensed Matter, 29.

Grenthe, I., Fuger, J., Konings, R.J.M., Lemire, R.J., Muller, A.B., Nguyen-Trung, C., and Wanner, H. (1993) Chemical thermodynamics of uranium. In Chemical Thermodynamics Vol. 1, p. 715.

Guo, X., Szenknect, S., Mesbah, A., Labs, S., Clavier, N., Poinssot, C., Ushakov, S. V., Curtius, H., Bosbach, D., Ewing, R.C., and others (2015) Thermodynamics of formation of coffinite, $USiO_4$. Proceedings of the National Academy of Sciences, 112, 6551–6555.

Guo, X., Szenknect, S., Mesbah, A., Clavier, N., Poinssot, C., Wu, D., Xu, H., Dacheux, N., Ewing, R.C., and Navrotsky, A. (2016) Energetics of a uranothorite ($Th_{1-x}U_xSiO_4$) solid solution. Chemistry of Materials, 28, 7117–7124.

Gysi, A.P., Williams-Jones, A.E., and Harlov, D. (2015) The solubility of xenotime-(Y) and other HREE phosphates ($DyPO_4$, $ErPO_4$ and $YbPO_4$) in aqueous solutions from 100 to 250°C and psat. Chemical Geology, 401, 83–95.

Gysi, A.P., Van Hoozen, C., and Harlov, D. (2021) Hydrothermal solubility of $TbPO_4$, $HoPO_4$, $TmPO_4$, and $LuPO_4$ xenotime endmembers at pH of 2 and temperatures between 100 and 250 °C. Chemical Geology, 567, 120072.

Hansley, P.L., and Fitzpatrick, J.J. (1989) Compositional and Crystallographic data on REE-bearing coffinite from the Grants uranium region, northwestern New Mexico. American Mineralogist, 74, 263–270.

Hazen, R.M., and Finger, L.M. (1979) Crystal structure and compressibility of zircon at high pressure. American Mineralogist, 64, 196–201.

Hirano, Y., Guedes, I., Grimsditch, M., Loong, C.K., Wakabayashi, N., and Boatner, L.A. (2002) Brillouin-scattering study of the elastic constants of $ErVO_4$. Journal of the American Ceramic Society, 85, 1001–1003.

Hoekstra, H.R., and Fuchs, L.H. (1956) Synthesis of coffinite - $USiO_4$. Science, 123, 105.

Huang, Z., Zhang, L., Feng, J., Cui, X., and Pan, W. (2012) Electronic, elastic and optical properties of zircon $GdVO_4$ investigated from experiments and LSDA + U. Journal of Alloys and Compounds, 538, 56–60.

Jiménez, E., Isasi, J., and Sáez-Puche, R. (2000) Synthesis, structural characterization and magnetic properties of $RCrO_4$ oxides, R = Nd, Sm, Eu and Lu. Journal of Alloys and Compounds, 312, 53–59.

——— (2002) Field-induced magnetic properties in $RCrO_4$ oxides (R = Pr, Gd, Tb, Tm, and Yb). Journal of Solid State Chemistry, 164, 313–319.

Kang, D.H., and Schleid, T. (2005) Einkristalle von $La[AsO_4]$ im monazit- und $Sm[AsO_4]$ im xenotim-typ. Zeitschrift fur Anorganische und Allgemeine Chemie, 631, 1799–1802.

Kang, D.-H., Hoss, P., and Schleid, T. (2005) Xenotime-type $Yb[AsO_4]$ Dong-Hee. Acta Crystallographica Section E: Structure Reports Online, 61, i270–i272.

Keller, V.C. (1963) Untersuchungen über die germanate und silikate des typs ABO_4 der vierwertigen elemente thorium bis americium. Nukleonik, 41–48.

Knittle, E., and Williams, Q. (1993) High-pressure raman spectroscopy of $ZrSiO_4$: observation of the zircon to scheelite transition at 300 K. American Mineralogist, 78, 245–252.

Knyazev, A. V., Komshina, M.E., and Savushkin, I.A. (2017) Synthesis and high-temperature X-ray diffraction study of thorium orthosilicate. Radiochemistry, 59, 225–228.

Konno, H., Aoki, Y., Klencsár, Z., Vértes, A., Wakeshima, M., Tezuka, K., and Hinatsu, Y. (2001) Structure of $EuCrO_4$ and its electronic and magnetic properties. Bulletin of the Chemical Society of Japan, 74, 2335–2341.

Kusaba, K., Syono, Y., Kikuchi, M., and Fukuoka, K. (1985) Shock behavior of zircon: phase transition to scheelite structure and decomposition. Earth and Planetary Science Letters, 72, 433–439.

Labs, S., Hennig, C., Weiss, S., Curtius, H., Zänker, H., and Bosbach, D. (2014) Synthesis of coffinite, $USiO_4$, and structural investigations of $U_xTh_{(1-x)}SiO_4$ solid solutions. Environmental Science and Technology, 48, 854–860.

Lacomba-Perales, R., Errandonea, D., Meng, Y., and Bettinelli, M. (2010) High-pressure stability and compressibility of APO_4(A=La, Nd, Eu, Gd, Er, and Y) orthophosphates: an x-ray diffraction study using synchrotron radiation. Physical Review B - Condensed Matter and Materials Physics, 81, 1–9.

Langmuir, D. (1978) Uranium solution-mineral equilibria at low temperatures with applications to sedimentary ore deposits. Geochimica et Cosmochimica Acta, 42, 547–569.

Langmuir, D., and Chatham, J.R. (1980) Groundwater prospecting for sandstone-type uranium deposits: a preliminary comparison of the merits of mineral-solution equilibria, and single-element tracer methods. Journal of Geochemical Exploration, 13, 201–219.

Ledderboge, F., Nowak, J., Massonne, H.J., Förg, K., Höppe, H.A., and Schleid, T. (2018) High-pressure investigations of yttrium(III) oxoarsenate(V): Crystal structure and luminescence properties of Eu^{3+}-doped scheelite-type $Y[AsO_4]$ from xenotime-type precursors. Journal of Solid State Chemistry, 263, 65–71.

Lee, Y.M., and Nassaralla, C.L. (2006) Standard free energy of formation of calcium chromate. Materials Science and Engineering A, 437, 334–339.

Li, H., Zhang, S., Zhou, S., and Cao, X. (2009) Bonding characteristics, thermal expansibility, and compressibility of RXO_4 (R = Rare Earths, X = P, As) within monazite and zircon structures. Inorganic Chemistry, 48, 4542–4548.

Li, H., Noh, H.M., Moon, B.K., Choi, B.C., and Jeong, J.H. (2014) Chemical bonding characterization, expansivity and compressibility of $RECrO_4$. Journal of Alloys and Compounds, 582, 151–156.

Li, K., Ding, Z., and Xue, D. (2011) Electronegativity-related bulk moduli of crystal materials. Physica Status Solidi (B) Basic Research, 248, 1227–1236.

Li, L., Yu, W., Long, Y., and Jin, C. (2006) First-principles calculations on the pressure induced zircon-type to scheelite-type phase transition of $CaCrO_4$. Solid State Communications, 137, 358–361.

Lohmüller, G., Schmidt, G., Deppisch, B., Gramlich, V., and Scheringer, C. (1973) Die kristallstrukturen von yttrium-vanadat, lutetium-phosphat und lutetium-arsenat. Acta Crystallographica Section B Structural Crystallography and Crystal Chemistry, 29, 141–142.

Long, F.G., and Stager, C. V. (1977) Low temperature crystal structure of $TbAsO_4$ and $DyAsO_4$. Canadian Journal of Physics, 55, 1633–1640.

Long, Y.W., Yang, L.X., You, S.J., Yu, Y., Yu, R.C., Jin, C.Q., and Liu, J. (2006) Crystal structural phase transition in $CaCrO_4$ under high pressure. Journal of Physics Condensed Matter, 18, 2421–2428.

Long, Y.W., Yang, L.X., Yu, Y., Li, F.Y., Yu, R.C., and Jin, C.Q. (2007) Synthesis, structure, magnetism and specific heat of $YCrO_4$ and its zircon-to-scheelite phase transition. Physical Review B - Condensed Matter and Materials Physics, 75, 1–7.

López-Solano, J., Rodríguez-Hernández, P., Muñoz, A., Gomis, O., Santamaría-Perez, D., Errandonea, D., Manjón, F.J., Kumar, R.S., Stavrou, E., and Raptis, C. (2010) Theoretical and experimental study of the structural stability of $TbPO_4$ at high pressures. Physical Review B - Condensed Matter and Materials Physics, 81, 1–9.

Marinova, L.A., Glibin, V.P., and Volkov, A.I. (1973) No Title. Rassh. Tezisi. Dokl. Tbilissi Meznierba.

Mazeina, L., Ushakov, S. V., Navrotsky, A., and Boatner, L.A. (2005) Formation enthalpy of $ThSiO_4$ and enthalpy of the thorite → huttonite phase transition. Geochimica et Cosmochimica Acta, 69, 4675–4683.

Mesbah, A., Clavier, N., Lozano-Rodriguez, M.J., Szenknect, S., and Dacheux, N. (2016) Incorporation of thorium in the zircon structure type through the $Th_{1-x}Er_x(SiO_4)_{1-x}(PO_4)_x$ thorite-xenotime solid solution. Inorganic Chemistry, 55, 11273–11282.

Mittal, R., Garg, A.B., Vijayakumar, V., Achary, S.N., Tyagi, A.K., Godwal, B.K., Busetto, E., Lausi, A., and Chaplot, S.L. (2008) Investigation of the phase stability of $LuVO_4$ at high pressure using powder x-ray diffraction measurements and latticedynamical calculations. Journal of Physics Condensed Matter, 20.

Mogilevsky, P., Zaretsky, E.B., Parthasarathy, T.A., and Meisenkothen, F. (2006) Composition, lattice parameters, and room temperature elastic constants of natural single crystal xenotime from Novo Horizonte. Physics and Chemistry of Minerals, 33, 691–698.

Mondal, S.K., Das, P.K., Mandal, N., and Arya, A. (2020) A novel approach to the structural distortions of U/Th snub-disphenoids and their control on zircon → reidite type phase transitions of $U_{1-x}Th_xSiO_4$. Journal of Physics Condensed Matter, 32.

Mrose, M.E., and Rose, J.Jr. (1961) Behierite,(Ta, Nb)BO_4, a new mineral from Manjaka, Madagascar. Geological Society of America, 111.

Mulak, J. (1977) Crystal field parameters in $USiO_4$ from temperature dependence of paramagnetic susceptibility. Journal of Solid State Chemistry, 21, 117–126.

Mullica, D.F., Sappenfield, E.L., Abraham, M.M., Chakoumakos, B.C., and Boatner, L.A. (1996) Structural investigations of several $LnVO_4$ compounds. Inorganica Chimica Acta, 248, 85–88.

Mursic, Z., Vogt, T., and Frey, F. (1992) High-temperature neutron powder diffraction study of $ZrSiO_4$ up to 1900 K. Acta Crystallographica Section B, 48, 584–590.

Navrotsky, A., and Ushakov, S. V (2005) Materials Fundamentals of Gate Dielectrics. Materials Fundamentals of Gate Dielectrics.

Ni, Y., Hughes, J.M., and Mariano, A.N. (1995) Crystal chemistry of the monazite and xenotime structures. American Mineralogist, 80, 21–26.

Ono, S., Tange, Y., Katayama, I., and Kikegawa, T. (2004) Equation of State of $ZrSiO_4$ phases in the upper mantle. American Mineralogist, 89, 185–188.

Panchal, V., López-Moreno, S., Santamaría-Pérez, D., Errandonea, D., Manjón, F.J., Rodríguez-Hernandez, P., Muñoz, A., Achary, S.N., and Tyagi, A.K. (2011) Zircon to monazite phase transition in $CeVO_4$: X-ray diffraction and Raman-scattering measurements. Physical Review B - Condensed Matter and Materials Physics, 84, 1–12.

Paszkowicz, W., Ermakova, O., López-Solano, J., Mujica, A., Muñoz, A., Minikayev, R., Lathe, C., Gierlotka, S., Nikolaenko, I., and Dabkowska, H. (2014) Equation of state of zircon- and scheelite-type dysprosium orthovanadates: A combined experimental and theoretical study. Journal of Physics Condensed Matter, 26.

Pointeau, V., Deditius, A.P., Miserque, F., Renock, D., Becker, U., Zhang, J., Clavier, N., Dacheux, N., Poinssot, C., and Ewing, R.C. (2009) Synthesis and characterization of coffinite. Journal of Nuclear Materials, 393, 449–458.

Popescu, C., Garg, A.B., Errandonea, D., Sans, J.A., Rodriguez-Hernández, P., Radescu, S., Muñoz, A., Achary, S.N., and Tyagi, A.K. (2016) Pressure-induced phase transformation in zircon-type orthovanadate $SmVO_4$ from experiment and theory. Journal of Physics Condensed Matter, 28.

Range, K.-J., Wildenauer, M., and Heyns, A.M. (1988) Extrem kurze nichtbindende Sauerstoff-Sauerstoff-Abstände: Die Kristallstrukturen von $NbBO_4$, $NaNb_3O_8$ und $NaTa_3O_8$. Angewandte Chemie, 100, 973–975.

Range, K.J., Wildenauer, M., and Andratshke, M. (1996) Crystal Structure of tantalum orthoborate, $TaBO_4$. Zeitschrift fur Kristallographie, 211, 815.

Reynolds, H.S. (2013) Synthesis, characterisation and dissolution studies of the uranium mineral coffinite. Royal Melbourne Institute of Technology University.

Robinson, K., Gibbs, G. V., and Ribbe, P.H. (1971) The structure of zircon: a comparison with garnet. American Mineralogist, 56, 782–790.

Ryumin, M.A., Gurevich, V.M., Khoroshilov, A. V., Tyurin, A. V., and Gavrichev, K.S. (2017) Heat capacity and thermodynamic functions of thulium orthophosphate $TmPO_4$ in the range of 10–1350 K. Russian Journal of Physical Chemistry A, 91, 2310–2316.

Sáez Puche, R., Gallardo, J.M., de Paz, R.J., Taira, N., and Climent-Pascual, E. (2009) Structural phase transitions zircon to scheelite type induced by pressure in the $RCrO_4$ oxides (R = rare earth). Journal of the Argentine Chemical Society, 97, 90–101.

Sáez-Puche, R., Jiménez, E., Isasi, J., Fernández-Díaz, M.T., and García-Muñoz, J.L. (2003) Structural and magnetic characterization of $RCrO_4$ oxides (R = Nd, Er and Tm). Journal of Solid State Chemistry, 171, 161–169.

Schafer, W., and Will, G. (1971) Neutron diffraction study of antiferromagnetic $DyAsO_4$. Journal of Physics C: Solid State Physics, 4, 3224–3233.

Schäfer, W., Will, G., and Müller-Vogt, G. (1979) Refinement of the crystal structure of terbium arsenate $TbAsO_4$ at 77 K and 5 K by profile analysis from neutron diffraction powder data. Acta Crystallographica Section B Structural Crystallography and Crystal Chemistry, 35, 588–592.

Schlüter, J., Malcherek, T., and Husdal, T.A. (2009) The new mineral stetindite, $CeSiO_4$, a cerium end-member of the zircon group. Neues Jahrbuch fur Mineralogie, Abhandlungen, 186, 195–200.

Schmidt, M., Müller, U., Gil, R.C., Milke, E., and Binnewies, M. (2005) Zum chemischen transport und zur kristallstruktur von seltenerdarsenaten(V). Zeitschrift fur Anorganische und Allgemeine Chemie, 631, 1154–1162.

Schuiling, R.D., Vergouwen, L., and van der Rijst, H. (1976) Gibbs energies of formation of zircon ($ZrSiO_4$), thorite($ThSiO_4$), and phenacite (Be_2SiO_4). American Mineralogist, 61, 166–168.

Shannon, R.D. (1976) Revised effective ionic radii and systematic studies of interatomic distances in halides and chalcogenides. Acta Crystallographica Section A, 32, 751–766.

Skakle, J.M.S., Dickson, C.L., and Glasser, F.P. (2000) The crystal structures of $CeSiO_4$ and $Ca_2Ce_8(SiO_4)_6O_2$. Powder Diffraction, 4, 234–238.

Speer, J.A., and Cooper, B.J. (1982) Crystal structure of synthetic hafnon, $HfSiO_4$, comparison with zircon and the actinide orthosilicates. American Mineralogist, 67, 804–808.

Stieff, L.R., Stern, T.W., and Sheerwood, A.M. (1956) Coffinite, A uranous silicate with hydroxyl subsitution: a new mineral. American Mineralogist, 41, 675–688.

Strzelecki, A.C., Bourgeois, C., Kriegsman, K.W., Estevenon, P., Wei, N., Szenknect, S., Mesbah, A., Wu, D., Ewing, R.C., Dacheux, N., and others (2020) Thermodynamics of $CeSiO_4$: implications for actinide orthosilicates. Inorganic Chemistry, 59, 13174–13183.

Strzelecki, A.C., Barral, T., Estevenon, P., Mesbah, A., Goncharov, V., Baker, J., Bai, J., Clavier, N., Szenknect, S., Migdissov, A., and others (2021) The role of water and hydroxyl groups in the structures of stetindite and coffinite, $MSiO_4$ (M = Ce, U). Inorganic Chemistry, 60, 718–735.

Strzelecki, A.C., Reece, M.E., Zhao, X., Yu, W., Benmore, C.J., Ren, Y., Alcorn, C.D., Migdisov, A., Xu, H., and Guo, X. (2022) Thermodynamics of mixing HREE in xenotime solid solution ($Er_{(x)}Yb_{(1-x)}PO_4$). ACS Earth and Space Chemistry, 4, 2461–2469.

Strzelecki, A.C., Zhao, X., Baker, J.L., Estevenon, P., Barral, T., Mesbah, A., Popov, D., Chariton, S., Prakapenka, V., Ahmed, S., Yoo, C.-S., and Guo, X. (2023) High-pressure structural and thermodynamic properties of cerium orthosilicates ($CeSiO_4$). The Journal of Physical Chemistry C, 127, 4225–4238.

Subbarao, E.C., Agrawal, D.K., McKinstry, H.A., Sallese, C.W., and Roy, R. (1990) Thermal expansion of compounds of zircon structure. Journal of the American Ceramic Society, 73, 1246–1252.

Szenknect, S., Costin, D.T., Clavier, N., Mesbah, A., Poinssot, C., Vitorge, P., and Dacheux, N. (2013) From uranothorites to coffinite: A solid solution route to the thermodynamic properties of $USiO_4$. Inorganic Chemistry, 52, 6957–6968.

Szenknect, S., Mesbah, A., Cordara, T., Clavier, N., Brau, H.P., Le Goff, X., Poinssot, C., Ewing, R.C., and Dacheux, N. (2016a) First experimental determination of the solubility constant of coffinite. Geochimica et Cosmochimica Acta, 181, 36–53.

——— (2016b) First experimental determination of the solubility constant of coffinite. Geochimica et Cosmochimica Acta, 181, 36–53.

Tananaev, I.V., Orlovsky, V.P., Kurbanov, J.M., Halikov, B.S., Osman, S.O., and Bulgakov, V.I. (1974) Reports of the Academy of Sciences of the Tajik SSR, 42 p.

Tange, Y., and Takahashi, E. (2004) Stability of the high-pressure polymorph of zircon ($ZrSiO_4$) in the deep mantle. Physics of the Earth and Planetary Interiors, 143, 223–229.

Taylor, M., and Ewing, R.C. (1978) The crystal structures of the $ThSiO_4$ polymorphs: huttonite and thorite. Acta Crystallographica Section B Structural Crystallography and Crystal Chemistry, 34, 1074–1079.

Tezuka, K., and Hinatsu, Y. (2001) Magnetic and crystallographic properties of $LnCrO_4$ (Ln=Nd, Sm, and Dy). Journal of Solid State Chemistry, 160, 362–367.

Tezuka, K., Doi, Y., and Hinatsu, Y. (2002) Crystal structures and magnetic properties of zircon-type compounds $Lu_{1-x}Y_xCrO_4$. Journal of Materials Chemistry, 12, 1189–1193.

Tyurin, A. V., Ryumin, M.A., Khoroshilov, A. V., Gurevich, V.M., and Gavrichev, K.S. (2020) Thermodynamic functions of holmium orthophosphate $HoPO_4$ in the range 9–1370 K. Thermochimica Acta, 683, 178459.

Ushakov, S. V., Helean, K.B., Navrotsky, A., and Boatner, L.A. (2001a) Thermochemistry of rare-earth orthophosphates. Journal of Materials Research, 16, 2623–2633.

——— (2001b) Thermochemistry of rare-earth orthophosphates. Journal of Materials Research, 16, 2623–2633.

Van Westrenen, W., Frank, M.R., Hanchar, J.M., Fei, Y., Finch, R.J., and Zha, C.-S. (2004) In situ determination of the compressibility of synthetic pure zircon ($ZrSiO_4$) and the onset of the zircon-reidite phase transformation. American Mineralogist, 89, 197–203.

Varghese, J., Joseph, T., Surendran, K.P., Rajan, T.P.D., and Sebastian, M.T. (2015) Hafnium silicate: a new microwave dielectric ceramic with low thermal expansivity. Dalton Transactions, 44, 5146–5152.

Wang, X., Loa, I., Syassen, K., Hanfland, M., and Ferrand, B. (2004) Structural properties of the zircon- and scheelite-type phases of YVO_4 at high pressure. Physical Review B - Condensed Matter and Materials Physics, 70, 3–8.

Weber, G., and Range, K.J. (1996) Notizen: die kristallstruktur von calciumchromat(VI), $CaCrO_4$ / the crystal structure of calcium chromate (VI), $CaCrO_4$. Zeitschrift für Naturforschung B, 51, 751–753.

Yue, B., Hong, F., Merkel, S., Tan, D., Yan, J., Chen, B., and Mao, H.K. (2016) Deformation behavior across the zircon-scheelite phase transition. Physical Review Letters, 117, 1–6.

Zhang, F.X., Lang, M., Ewing, R.C., Lian, J., Wang, Z.W., Hu, J., and Boatner, L.A. (2008) Pressure-induced zircon-type to scheelite-type phase transitions in $YbPO_4$ and $LuPO_4$. Journal of Solid State Chemistry, 181, 2633–2638.

Zhang, F.X., Pointeau, V., Shuller, L.C., Reaman, D.M., Lang, M., Liu, Z., Hu, J., Panero, W.R., Becker, U., Poinssot, C., and others (2009a) Structural transitions and electron transfer in coffinite, $USiO_4$, at high pressure. American Mineralogist, 94, 916–920.

——— (2009b) Structural transitions and electron transfer in coffinite, $USiO_4$, at high pressure. American Mineralogist, 94, 916–920.